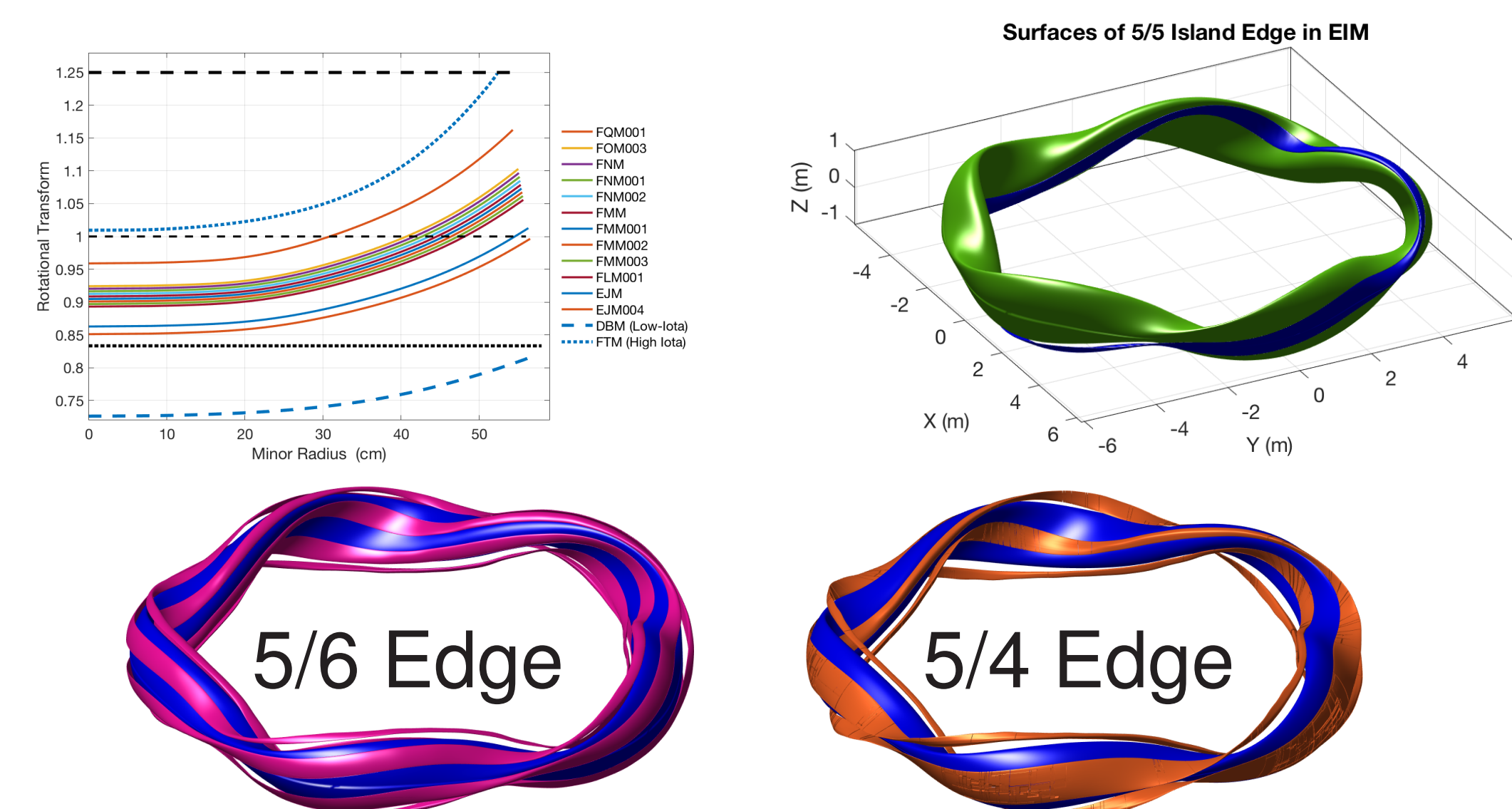


ABSTRACT

The edge island domain in Wendelstein 7-X consists of divertor islands that coincide with the location of rational values of the rotational transform $\iota \approx (5/6, 5/5, 5/4)$ and surround the main confinement volume (the ‘main plasma’). The ‘5/5’ edge is 5 individual islands that are unconnected. In contrast, a single island connects onto itself after 6 or 4 toroidal transits in the ‘5/6’ and ‘5/4’ edge, respectively. Many interesting phenomena are related to these islands and diagnostic analyses require a mapping from ‘laboratory’ or real space coordinates to the island coordinate system. Two procedures are described here to calculate several scalar and vector quantities for closed island structures which can be utilized in fast interpolation schemes for inverse maps. For the ‘5/5’ edge, a fixed-boundary vacuum (zero beta) magneto-hydrodynamic solutions of the 5/5 island is found with VMEC. The solution is compatible with already existing routines which determine $\nabla\psi_{toroidal}$ (and other quantities) of VMEC solutions at arbitrary laboratory coordinates via stellarator symmetry. VMEC does not support solutions for the 5/4 and 5/6 island cases, but the $\nabla\psi_{toroidal}$ and $\mathbf{B} \times \nabla\psi_{toroidal}$ vectors can be constructed directly or from a 2-D Fourier series representation.

EDGE ISLAND DOMAINS

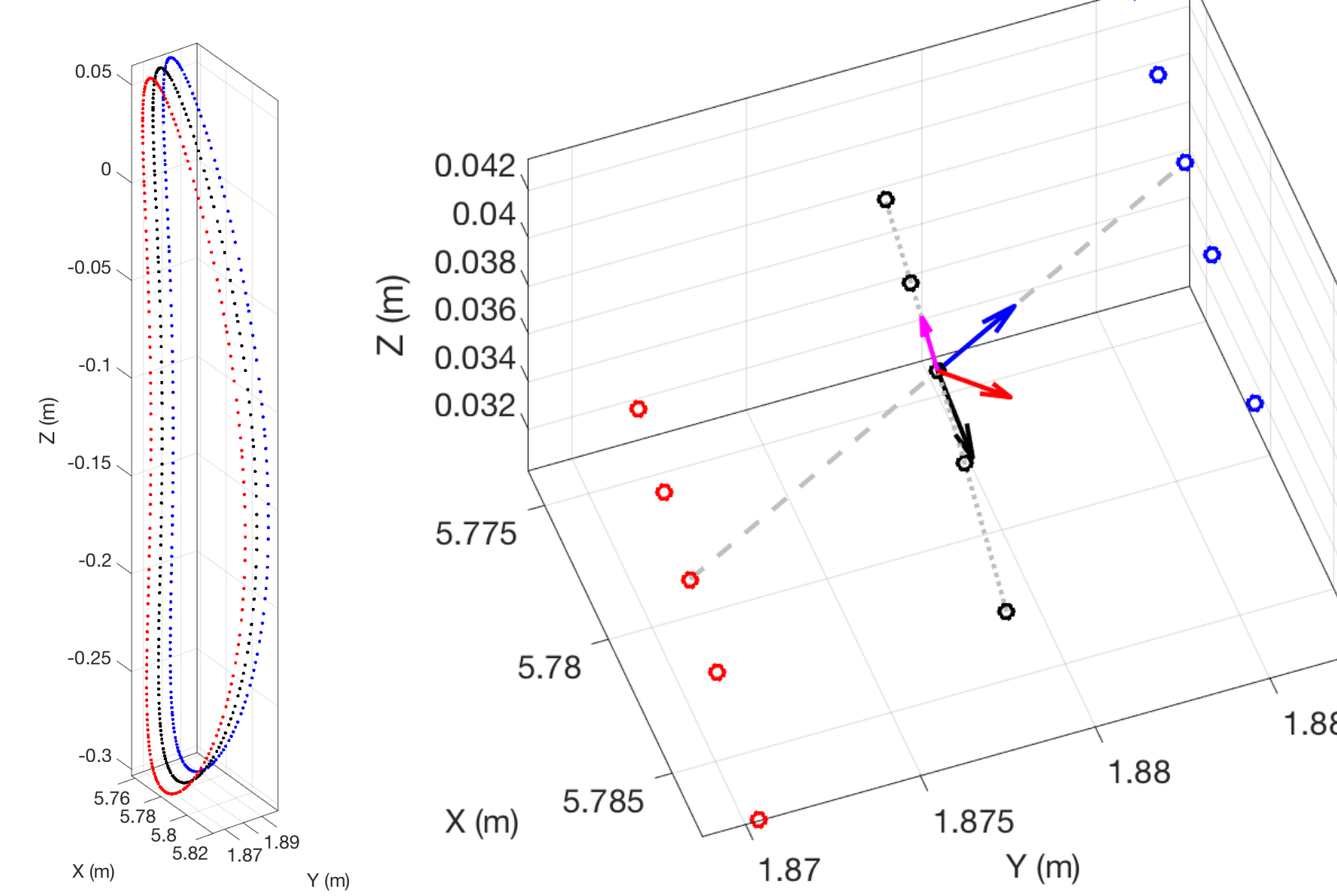
The rotational transform at the edge of the plasma column can be varied with coil current to be resonant with $\iota \approx 5/6, 5/5$, or $5/4$.



SURFACE GENERATION

Field-line following is the primary tool for generating surfaces:

$$\frac{\vec{B}}{dl} = \frac{B_x}{dx} = \frac{B_y}{dy} = \frac{B_z}{dz}$$



Left: Three Poincaré maps (red, black and blue points) generated from field-line following for a surface in the 5/6 island region of W7-X.

Right: A subset of points (shown now as red, black and blue open circles)

- \mathbf{V}_1 (magenta) is formed by the two neighboring points in the poloidal direction at constant toroidal angle, along the dotted black line.
- \mathbf{V}_2 (blue) points along the (dashed black) line that connects points in neighboring toroidal Poincaré maps, \parallel to \mathbf{B} .
- $\nabla\psi$ (red) is the outward normal vector
- The binormal vector is: $\hat{\mathbf{b}} = (\mathbf{B} \times \nabla\psi) / (|\mathbf{B}||\nabla\psi|)$ (black)

Poincaré maps at uniformly sampled planes at toroidal angle $\phi'(i)$ are described by a set of poloidal harmonics,

$$\phi'(i) = \frac{2\pi(i-1)}{N_\phi N_{FP}}, i \in 1 \dots N_\phi$$

$$R(\phi', \rho) = \sum_{m=0}^{M_{Pol}} R_{m,c}(\phi', \rho) \cos(2\pi m\theta) + R_{m,s}(\phi', \rho) \sin(2\pi m\theta)$$

$$Z(\phi', \rho) = \sum_{m=0}^{M_{Pol}} Z_{m,c}(\phi', \rho) \cos(2\pi m\theta) + Z_{m,s}(\phi', \rho) \sin(2\pi m\theta)$$

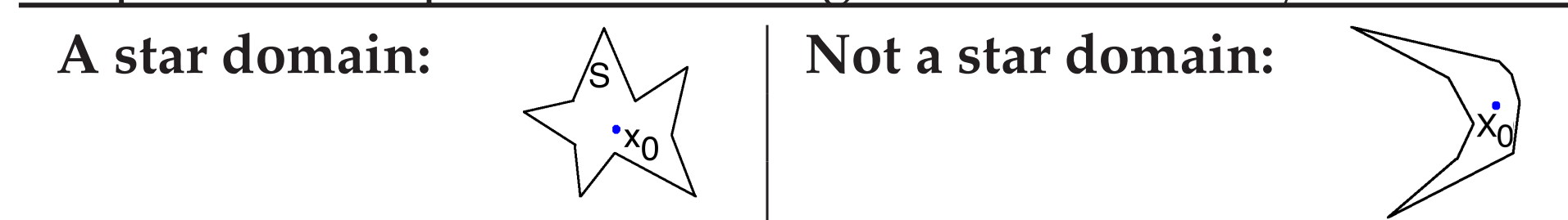
The poloidal angle, θ is unspecified at this point: Polar, quasi-polar, arclength, or other schemes can be used. For each Poincaré map:

- Points are sorted and assigned a poloidal angle, $\theta' \in [0, 2\pi]$, such that the points along the curve are monotonically increasing as a function of arclength from any fixed point along the curve.

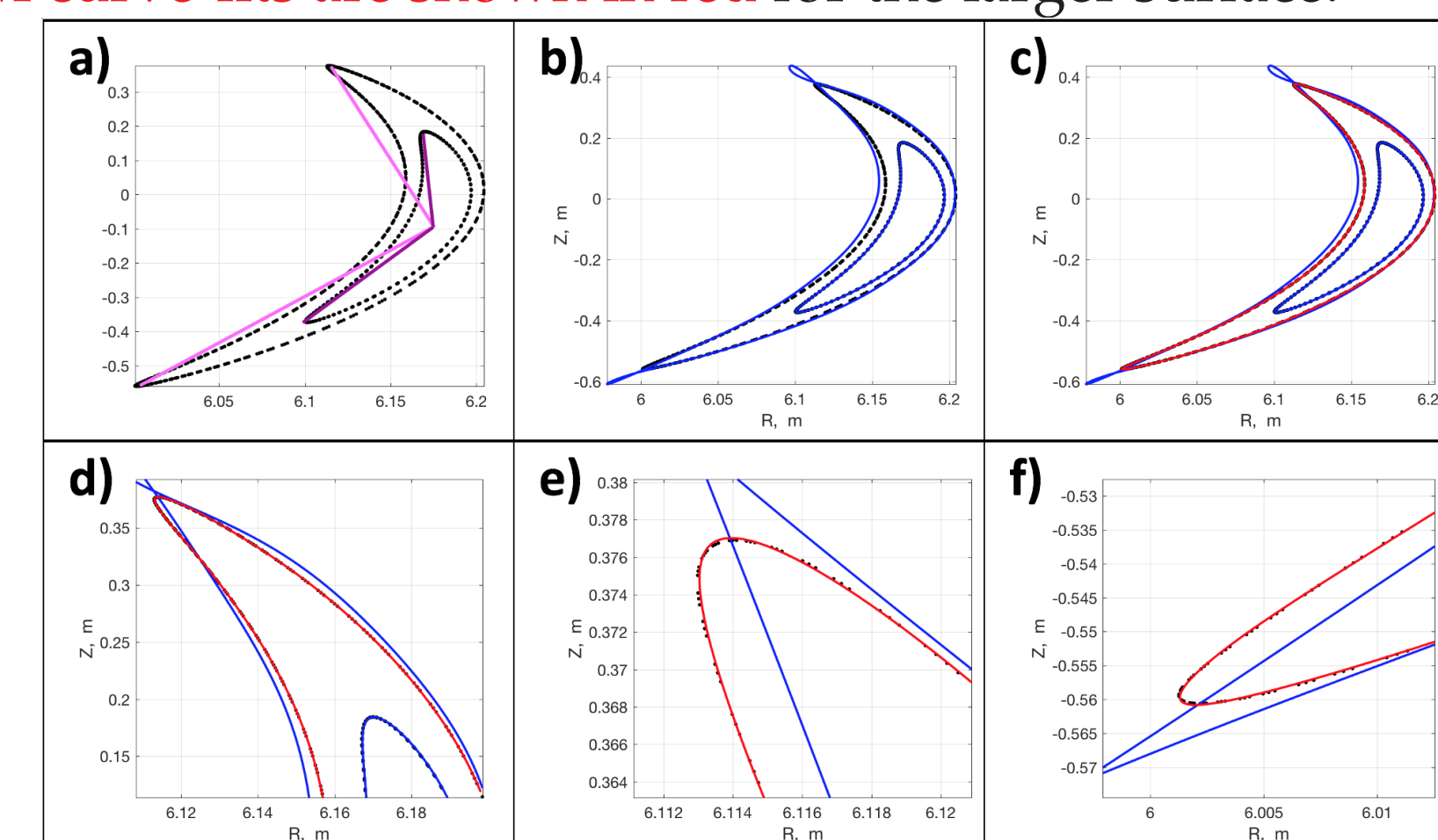
- A polar axis enclosed with the surface is identified for each map.
- The angle θ' is adjusted for each map to optimize for $M = 1$ modes so that $Z_{1,n,s} = Z_{1,-n,s}$ and $Z_{1,n,c} = Z_{1,-n,c}$.

In later stages, θ' can be further optimized, if desired.

A set S in Euclidean space \mathbf{R}^2 is called a star domain if there exists a point x_0 in S such that for all $x \in S$ the line segment from x_0 to x is in S . In this specific example, x_0 is the magnetic axis of the 5/5 island.



Poincaré maps (points in black) and the 2-D Fourier curve-fits at $\phi = -2\pi/90$ in the configuration FLM. Magenta lines in (a) demonstrate that the smaller surface is a star domain while the larger surface is not a star domain. In (b) - (f), DESCUR curve-fits are shown in blue for two surfaces and L-M curve-fits are shown in red for the larger surface.



SURFACE GENERATION, CONT

2-D Fourier spectrum is formed from the individual $(R_{m,c}(\phi', \rho), R_{m,s}(\phi', \rho), Z_{m,c}(\phi', \rho), Z_{m,s}(\phi', \rho))$ spectral components at each toroidal angle $\phi'(i)$:

$$R_{m,n,c}(\rho) = \frac{1}{N_\phi} \sum_{i=1}^{N_\phi} [R_{m,c}(\phi', \rho) \cos(n\phi' N_{FP}) + R_{m,s}(\phi', \rho) \sin(n\phi' N_{FP})]$$

$$R_{m,n,s}(\rho) = \frac{1}{N_\phi} \sum_{i=1}^{N_\phi} [R_{m,s}(\phi', \rho) \cos(n\phi' N_{FP}) - R_{m,c}(\phi', \rho) \sin(n\phi' N_{FP})]$$

$$Z_{m,n,c}(\rho) = \frac{1}{N_\phi} \sum_{i=1}^{N_\phi} [Z_{m,c}(\phi', \rho) \cos(n\phi' N_{FP}) + Z_{m,s}(\phi', \rho) \sin(n\phi' N_{FP})]$$

$$Z_{m,n,s}(\rho) = \frac{1}{N_\phi} \sum_{i=1}^{N_\phi} [Z_{m,s}(\phi', \rho) \cos(n\phi' N_{FP}) - Z_{m,c}(\phi', \rho) \sin(n\phi' N_{FP})]$$

$$R_{0,0,c}(\rho) = \frac{2}{N_\phi} \sum_{i=1}^{N_\phi} R_{0,c}(\phi'(i), \rho) \quad R_{0,0,s}(\rho) = \frac{2}{N_\phi} \sum_{i=1}^{N_\phi} R_{0,s}(\phi'(i), \rho)$$

$$Z_{0,0,c}(\rho) = \frac{2}{N_\phi} \sum_{i=1}^{N_\phi} Z_{0,c}(\phi'(i), \rho) \quad Z_{0,0,s}(\rho) = \frac{2}{N_\phi} \sum_{i=1}^{N_\phi} Z_{0,s}(\phi'(i), \rho)$$

- Boundary definitions derived from this method include a rotating ellipse in the spectrum, have a rotational transform $\iota \approx 1$ and poor numerical (VMEC) convergence.
- The following adjustment of the spectrum is made to remove the global transform (≈ 1) and resulted in MHD equilibria with $\iota \approx 0$ and better numerical convergence.

$$\theta \rightarrow \theta^*$$

$$n \rightarrow (n - m)$$

such that

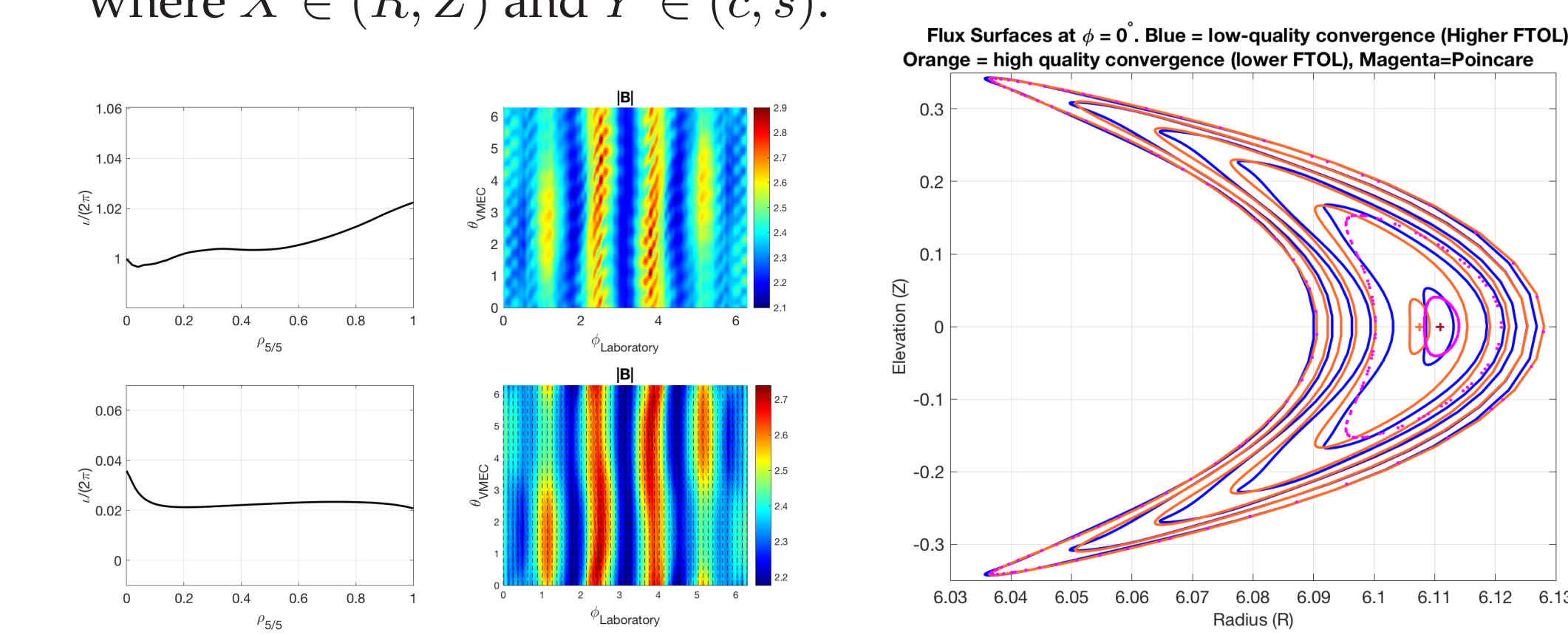
$$m\theta + n\phi \rightarrow m\theta^* + (n - m)\phi$$

- The $m = 0$ modes are unchanged. The $m \geq 1$ modes are remapped. Two examples are shown here:

$$X_{m=5,n=45,Y} \rightarrow X_{m=5,n=40,Y}$$

$$X_{m=6,n=-45,Y} \rightarrow X_{m=6,n=-51,Y}$$

where $X \in (R, Z)$ and $Y \in (c, s)$.



Left: Rotational transform for $\iota \sim 1$ (top) and $\iota \sim 0$ (bottom) configuration. Middle: $|\mathbf{B}|$ on the LCFS for the two configurations. Right: Surfaces from Poincaré Map (magenta), $\iota \sim 1$ (blue) and $\iota \sim 0$ (red).

HE-BEAM T_e CONTOURS

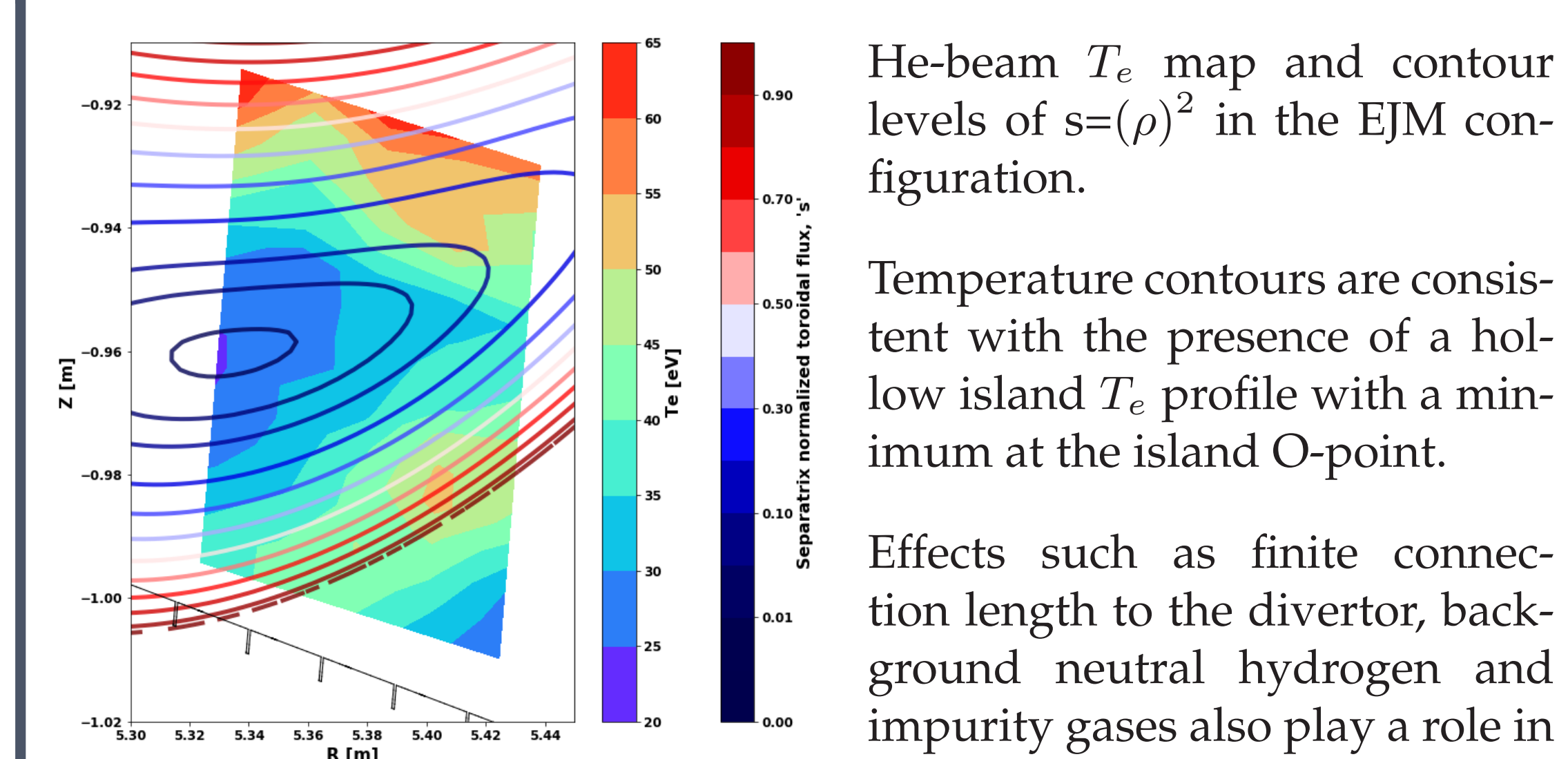
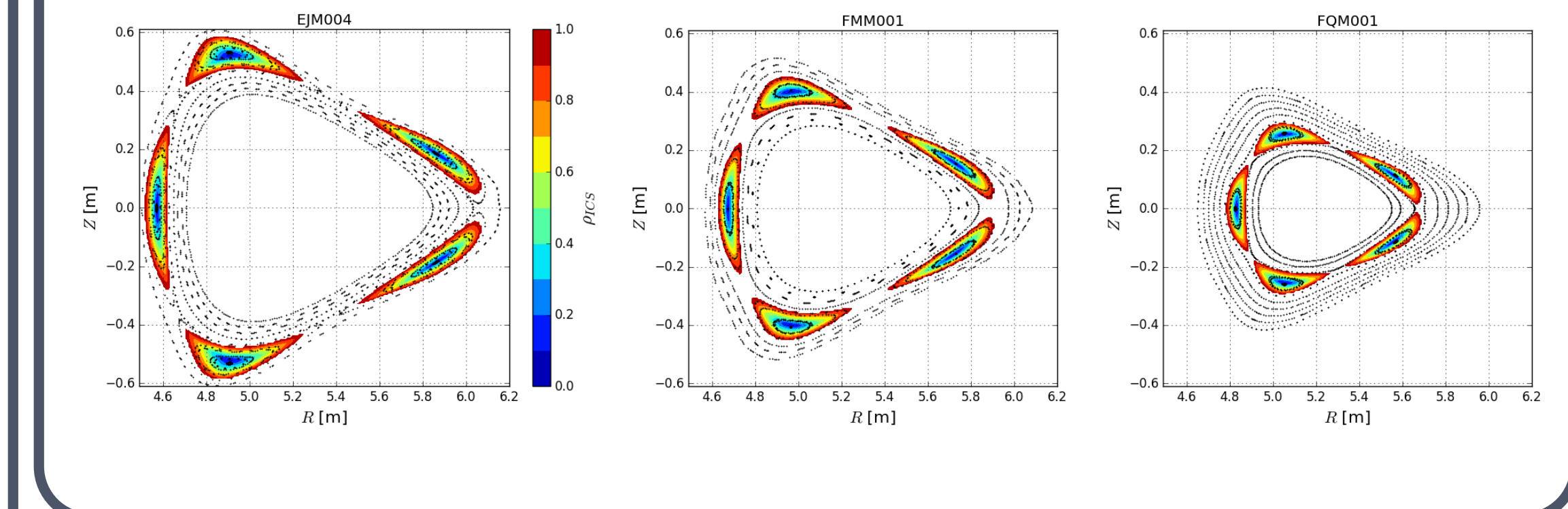


Figure courtesy E. Flom (Univ-Wisc).

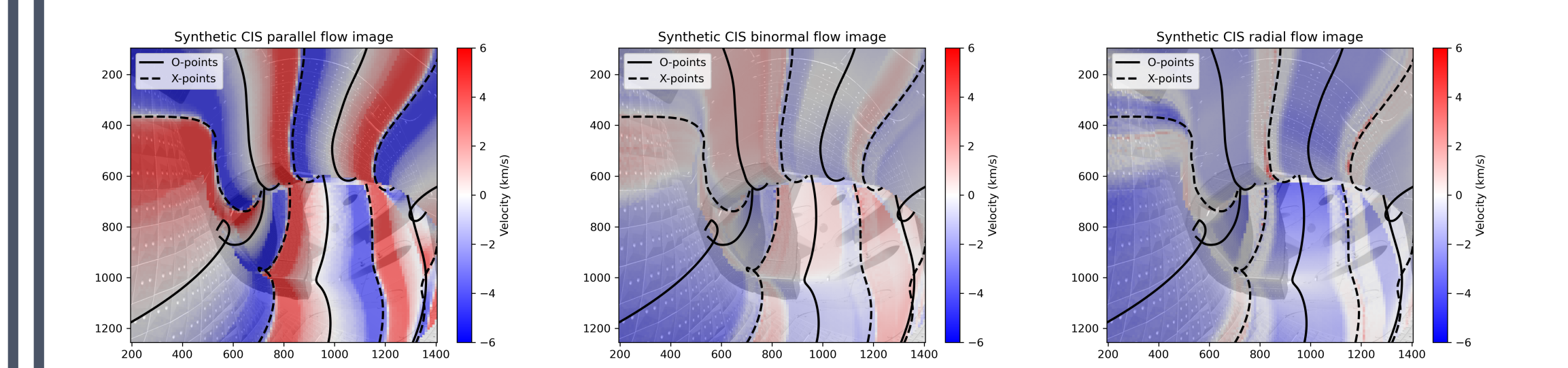
See poster PP11.00076.

IOTA RESONANCE SCAN WITH $\iota_{edge} \sim 1$

Maps of ρ_{ICS} at the 1/2-field period location for a subset of configurations from the Iota Scan, Session 53. Poincaré maps for each configuration are shown as black points.



COHERENCE IMAGING SPECTROSCOPY



Synthetic flow images for the W7-X coherence imaging spectroscopy diagnostic assuming a purely parallel (left), binormal (middle), or radial (right) flow in the island SOL. The trajectories of the island O-points (solid black lines) and X-points (dashed black lines) are overplotted.

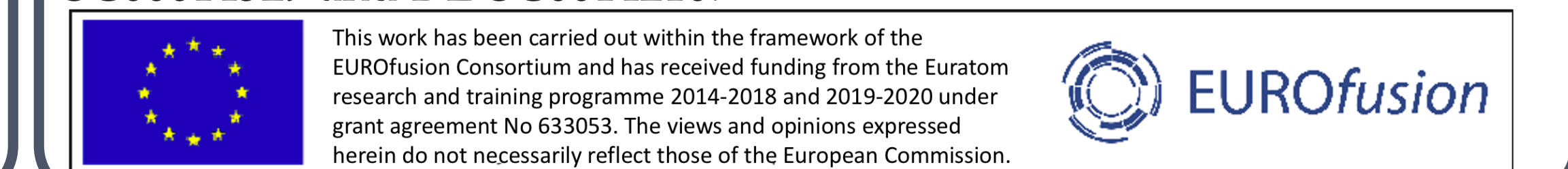
Figure courtesy M. Kriete (AU). See poster PP11.00064.

CONCLUSION

- Primarily intended as a tool for spectroscopic data interpretation in edge plasma domain.
 - Traditional MHD solutions (VMEC) don't include the edge islands.
 - $\mathbf{E} \times \mathbf{B}$ flows align with the binormal direction.
 - Interesting phenomena related to these islands and diagnostic analyses require a mapping from ‘laboratory’ or real space coordinates to the island coordinate system.
 - Can calculate scalar and vector quantities for closed island structures and can be utilized in fast interpolation schemes for inverse maps.
- A VMEC MHD solution for isolated islands
 - W7-X with $\iota_{edge} \approx 1$ (5/5)
 - Requires an increased toroidal mode spectrum range in the VMEC equilibrium.
- The Webservices VMEC mapping routines can be used to correlate observations at disparate viewing locations for the 5/5 islands
 - Compare flux surface quantities at different positions where surfaces have vastly different shapes
 - Iota scan edge measurements
 - In addition to correlations in the mean values, look for correlations in the fluctuation spectra. (Slow /Fast fluctuations, bursts or other solitary events.)
 - The truncated toroidal spectrum can limit the quality of the VMEC solution, if too few terms are allowed.
- For the 5/6 and 5/4 islands, Poincaré and \mathbf{B} data can be used to construct the vector maps or they can be calculated from the 2-D Fourier representation.

SUPPORT

This work is supported by U.S. Department of Energy grants DE-SC00014529 and DE-SC0014210.



BOUNDARY DEFINITIONS

Islands that close after a single toroidal transit (5/5 edge) have a boundary described by a 2-D Fourier series. θ is a poloidal angle, $\zeta \equiv \phi$ is the (laboratory) toroidal angle. The poloidal and toroidal modes numbers are m and n , respectively.

$$R(\rho, \theta, \zeta) = \sum_m \sum_n R_{m,n,c}(\rho) \cos(m\theta - nN\zeta) + \sum_m \sum_n R_{m,n,s}(\rho) \sin(m\theta - nN\zeta)$$

$$Z(\rho, \theta, \zeta) = \sum_m \sum_n Z_{m,n,c}(\rho) \cos(m\theta - nN\zeta) + \sum_m \sum_n Z_{m,n,s}(\rho) \sin(m\theta - nN\zeta)$$

$$\phi(\rho, \theta, \zeta) = \zeta$$

The 2-D Fourier spectrum is truncated:

$$0 \leq m \leq (M_{Pol} - 1)$$

$$-N_{Tor} \leq n \leq N_{Tor}$$

Islands that close after multiple toroidal transits (5/6 and 5/4 edges) have an analogous set of equations. Suppose F_M is the number of times the flux tube traverses in the toroidal direction around the torus until it closes upon itself. Two auxiliary toroidal-like angles are defined:

$$\alpha \in [0, F_M * 2\pi]$$

$$\text{mod}(\alpha, 2\pi) = \phi$$

$$\gamma \in [0, 2\pi] = \alpha / F_M$$

$$R(\rho, \theta, \gamma) = \sum_m \sum_n R_{m,n,c}(\rho) \cos(m\theta - n\gamma) + \sum_m \sum_n R_{m,n,s}(\rho) \sin(m\theta - n\gamma) \quad (1)$$

$$Z(\rho, \theta, \gamma) = \sum_m \sum_n Z_{m,n,c}(\rho) \cos(m\theta - n\gamma) + \sum_m \sum_n Z_{m,n,s}(\rho) \sin(m\theta - n\gamma) \quad (2)$$

$$\phi(\rho, \theta, \gamma) = \text{mod}(\gamma * F_M, 2\pi)$$

The laboratory toroidal angle of ϕ_X corresponds to F_M angles in γ , specifically:

$$\gamma_{1 \dots F_M} = \phi_X / F_M, (\phi_X + 2\pi) / F_M, \dots, (\phi_X + (F_M - 1)2\pi) / F_M$$

RADIAL AND BINORMAL VECTORS

Derivatives of $X \in (R, Z)$ with respect to ρ, θ, ζ and γ are written as:

$$dX/d\rho \equiv X_\rho = \sum_m \sum_n \frac{\partial X_{m,n,c}(\rho)}{\partial \rho} \cos(m\theta - n\zeta) + \sum_m \sum_n \frac{\partial X_{m,n,s}(\rho)}{\partial \rho} \sin(m\theta - n\zeta)$$

$$dX/d\theta \equiv X_\theta = \sum_m \sum_n -m X_{m,n,c} \sin(m\theta - n\zeta) + \sum_m \sum_n m X_{m,n,s} \cos(m\theta - n\zeta)$$

$$dX/d\zeta \equiv X_\zeta = \sum_m \sum_n n X_{m,n,c} \sin(m\theta - n\zeta) - \sum_m \sum_n n X_{m,n,s} \cos(m\theta - n\zeta)$$

$$dX/d\gamma \equiv X_\gamma = \sum_m \sum_n n X_{m,n,c} \sin(m\theta - n\gamma) - \sum_m \sum_n n X_{m,n,s} \cos(m\theta - n\gamma)$$

For the islands that connect after a single toroidal transit, the volume, toroidal flux and radial derivative are defined as

$$V(\rho') = \int_{\rho=0}^{\rho'} \int_{\theta=0}^{2\pi} \int_{\zeta=0}^{2\pi} d\rho d\theta d\zeta \sqrt{g}$$

$$\psi(\rho') = \int_{\rho=0}^{\rho'} \int_{\theta=0}^{2\pi} d\rho d\theta (\vec{\mathbf{B}} \cdot d\zeta)$$

$$\frac{dV}{d\rho} = 4\pi^2 < \sqrt{g} >$$

$$\frac{\partial V}{\partial \rho} = \int_{\theta=0}^{2\pi} \int_{\zeta=0}^{2\pi} d\theta d\zeta \sqrt{g}$$

$$\nabla\psi \sqrt{g} = -Z_\theta \hat{\mathbf{R}} + (R_\zeta Z_\theta - R_\theta Z_\zeta) \hat{\boldsymbol{\phi}} + R_\theta \hat{\mathbf{Z}}$$

$$\sqrt{g} = R(Z_\rho R_\theta - R_\rho Z_\theta)$$

For the islands that connect after multiple toroidal transits,

$$V(\rho') = \int_{\rho=0}^{\rho'} \int_{\theta=0}^{2\pi} \int_{\gamma=0}^{2\pi} d\rho d\theta d\gamma \sqrt{g}$$

$$\psi(\rho') = \int_{\rho=0}^{\rho'} \int_{\theta=0}^{2\pi} d\rho d\theta (\vec{\mathbf{B}} \cdot d\gamma)$$

$$\frac{\partial V}{\partial \rho} = \int_{\theta=0}^{2\pi} \int_{\gamma=0}^{2\pi} d\theta d\gamma \sqrt{g}$$

$$\nabla\psi \sqrt{g} = -Z_\theta \hat{\mathbf{R}} + (R_\gamma Z_\theta - R_\theta Z_\gamma) \hat{\boldsymbol{\gamma}} + R_\theta \hat{\mathbf{Z}}$$

$$\sqrt{g} = R(Z_\rho R_\theta - R_\rho Z_\theta)$$

For both cases, $\nabla\psi$ is combined with the local value of $\hat{\mathbf{t}} \equiv \vec{\mathbf{B}}/|\vec{\mathbf{B}}|$ to form the binormal vector $\hat{\mathbf{b}} \equiv \hat{\mathbf{t}} \times \nabla\psi/|\nabla\psi|$.

REFERENCES

- [1] S.P. Hirshman and J.C. Whitson. Steepest-descent moment method for three-dimensional mhd equilibria. *Phys. Fluids*, 26:3553–3568, 1983.
- [2] S.P. Hirshman and H.K. Meier. Optimized fourier representations for three-dimensional magnetic surfaces. *Phys. Fluids*, 28, 1985.